ENTANGLED STATES OF ATOMIC IONS.
FOR QUANTUM METROLOGY AND COMPUTATION[†]

D.J. WINELAND, C. MONROE, D.M. MEEKHOF, B.E. KING, D. LEIBFRIED,
W.M. ITANO, J.C. BERGQUIST, D. BERKELAND, J.J. BOLLINGER, J. MILLER
Ion Storage Group, Time and Frequency Division, NIST, Boulder, CO, 80303, USA

A single trapped $^9Be^+$ ion is used to investigate Jaynes-Cummings dynamics for a two-level atomic
system coupled to harmonic atomic motion. We create and investigate nonclassical states of motion
including "Schrödinger-cat" states. A fundamental quantum logic gate is realized using the quantized
motion and internal states as qubits. We explore some of the applications for, and problems in
realizing, quantum logic based on multiple trapped ions.

1   Introduction

Currently, a major theme in atomic physics is coherent control of quantum states. This
theme is manifested in a number of topics such as atom interferometry, atom optics, the
atom laser, Bose-Einstein condensation, cavity-QED, electromagnetic-induced
transparency, lasing without inversion, quantum computation, quantum cryptography,
quantum-state engineering, squeezed states, and wavepacket dynamics. A number of these
topics are the subjects of other presentations at this meeting.

In this paper we report related trapped-ion research on (1) the study of Jaynes-
Cummings dynamics for a two-level atomic system coupled to harmonic atomic motion, (2)
the study of quantum mechanical measurement problems such as the generation of
Schrödinger-cat-like superposition states and their relation to various decoherence
phenomena, and (3) coherent quantum logic for the investigation of scaling in a quantum
computer and for preparation of entangled states useful for spectroscopy.

2   Entanglement

An entangled quantum state is one where the wave function of the overall system cannot be
written as a product of the wave functions of the subsystems. In this case, a measurement
on one of the subsystems will affect the state of the other subsystems. For example,
consider a two-level atom bound in a 1-D harmonic well. Suppose we can create the state

$$\Psi = \frac{1}{\sqrt{2}}(|\downarrow\rangle|n\rangle + e^{i\phi}|\uparrow\rangle|n'\rangle),\tag{1}$$

where the kets $|\downarrow\rangle$ and $|\uparrow\rangle$ denote the two internal eigenstates of the atom (here, we use the
spin-½ analog to a two-level system: $\sigma_z|\uparrow\rangle = +|\uparrow\rangle$, etc.), the second ket denotes a harmonic
oscillator eigenstate $|n\rangle$, and ϕ is a (controlled) phase factor. If we measure the motional
eigenstate of the atom and find it to be in level n, then it must also be found in the $\downarrow$ internal
state if we measure σ_z. Similarly, if we find the atom in the n' motional state, it must be

31

found in the ↑ internal state. Such correlations are at the heart of the "EPR" experiments[1]. Another state we will consider below is the state for N two-level atoms

$$\Psi = \frac{1}{\sqrt{2}} (|\downarrow\rangle_1 |\downarrow\rangle_2 ... |\downarrow\rangle_N + e^{i\phi} |\uparrow\rangle_1 |\uparrow\rangle_2 ... |\uparrow\rangle_N) , \qquad (2)$$

where the subscript i (= 1, 2, ..., N) denotes the ith atom. This state is "maximally entangled" in the sense that a measurement of σ_z on any atom automatically determines the value of σ_z of all other atoms.

3 Jaynes-Cummings-type coupling between internal and motional states

To achieve entanglement from an initially nonentangled system, we need to provide a coupling between subsystems so that the state of one subsystem affects the dynamics of another. Coupling between spins or two-level atoms can, in principle, be achieved through a dipole-dipole interaction (like the hyperfine coupling between electron and proton in the hydrogen atom). In a system of trapped neutral atoms, dipole-dipole coupling may be difficult to control to the desired level; for trapped ions the Coulomb repulsion inhibits strong dipole coupling between ions. However, in the case of trapped ions, the motion can be strongly coupled to the internal levels with the application of inhomogeneous (classical) electromagnetic fields. For example, we consider an atom confined in a 1-D harmonic potential. The atom's dipole moment μ is assumed to couple to an electric field E(x,t) through the Hamiltonian

$$H_I = -\mu E(x,t) = -\mu \left[E(x=0,t) + \frac{\partial E}{\partial x} x + \frac{1}{2} \frac{\partial^2 E}{\partial x^2} x^2 + \cdots \right]. \qquad (3)$$

We have $\mu \propto \sigma_+ + \sigma_-$, where σ_+ and σ_- are the raising and lowering operators for the internal levels (in the spin-½ analog). In Eq. (3), the position x is an operator which we write as x = $x_o(a + a^\dagger)$, where a and $a^\dagger$ are the usual harmonic oscillator lowering and raising operators, and x_o is the rms spread of the n=0 zero-point state of motion. As a simple example, suppose the field is static and the motional oscillation frequency ω of the atom is equal to the resonance frequency ω_o of the internal state transition. In its reference frame, the atom experiences an oscillating field due to the motion through the inhomogeneous field. Since $\omega = \omega_o$, this field resonantly drives transitions between the internal states. If the extent of the atom's motion is small enough that we need only consider the first two terms in Eq. (3), H_I can be approximated as $H_{JCM} = \hbar\Omega(\sigma_+ a + \sigma_- a^\dagger)$ (in the interaction frame and using the rotating wave approximation) where Ω is a proportionality constant. This Hamiltonian is also obtained if E is sinusoidally time varying (frequency ω_L) and we satisfy the resonance condition $\omega_L + \omega = \omega_o$. This type of coupling was used to couple the spin and cyclotron motion in the classic electron g - 2 experiments of Dehmelt and coworkers[2]. Formally it is equivalent to the Jaynes-Cummings Hamiltonian of cavity-QED[3,4] which describes the

coupling between a two-level atom and a single mode of the radiation field. This analogy has been pointed out in various papers[5-8]; for a review, see Ref. 9 and further references in Ref. 8.

3.1 Realization a Jaynes-Cummings-type coupling for a trapped $^9Be^+$ ion

To controllably manipulate the internal and vibrational levels of the ion, we must (1) initialize the ion in a well defined internal and motional state and (2) make the vibrational level spacing (trap frequency) much larger than any internal or motional relaxation rates. To accomplish this, we have built an rf (Paul) ion trap which confines a single $^9Be^+$ ion with pseudopotential harmonic trap frequencies of $(\omega_x, \omega_y, \omega_z)/2\pi \approx (11, 19, 29)$ MHz along the three principal axes of the trap[10].

The energy-level structure of $^9Be^+$ is summarized in Fig. 1. Because the ion is harmonically bound, the internal $^9Be^+$ electronic states must include the ladder of external harmonic oscillator levels of energy $E_n = \hbar\omega(n+\frac{1}{2})$, where we have considered only the x-dimension of the oscillator ($\omega \equiv \omega_x$) and its associated quantum number $n \equiv n_x \in (0, 1, 2, ...)$. The two internal levels of interest are the $^2S_{1/2}$ ground state hyperfine levels $|F=2, m_F=2\rangle$ (denoted by $|\downarrow\rangle$) and $|F=1, m_F=1\rangle$ (denoted by $|\uparrow\rangle$), which are separated in frequency by $\omega_0/2\pi \approx 1.25$ GHz. The other Zeeman levels are resolved from the $|\downarrow\rangle$ and $|\uparrow\rangle$ states by the application of a ≈ 0.2 mT magnetic field[8,11].
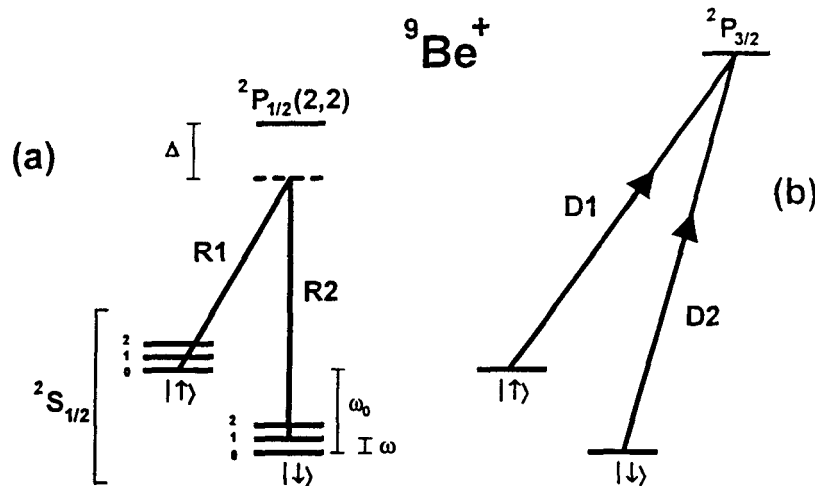

Fiq. 1. (a) Electronic (internal) and motional (external) energy levels (not to scale) of the trapped $^9Be^+$ ion, coupled by indicated laser beams R1 and R2. The difference frequency of the Raman beams R1 and R2 is set near $\omega_0/2\pi \approx$ 1.250 GHz, providing a two-photon Raman coupling between the $^2S_{1/2}(F=2, m_F=2)$ and $^2S_{1/2}(F=1, m_F=1)$ hyperfine ground states (denoted by $|\downarrow\rangle$ and $|\uparrow\rangle$ respectively). The motional energy levels are depicted by a ladder of vibrational states separated in frequency by the trap frequency $\omega/2\pi \approx 11$ MHz. The Raman beams are detuned $\Delta/2\pi \approx -12$ GHz from the $^2P_{1/2}(F=2, m_F=2)$ excited state. As shown, the Raman beams are tuned to the red sideband. (b) Detection of the internal state is accomplished by illuminating the ion with σ^+-polarized "detection" beam D2, which drives the cycling $^2S_{1/2}(F=2, m_F=2) \rightarrow {}^2P_{3/2}(F=3, m_F=3)$ transition, and observing the scattered fluorescence. The vibrational structure is omitted from (b) since it is not resolved. Beam D1, also σ^+ polarized, provides spontaneous recycling from the $|\uparrow\rangle$ to $|\downarrow\rangle$ state.

Strong field gradients can be obtained with laser fields (e^{ikx} factor). In our experiment, the field corresponding to that in Eq. (3) is provided by two laser fields which drive stimulated-Raman transitions between the levels of interest (R1 and R2 of Fig. 1a). (The use of stimulated-Raman transitions has some technical advantages, but is formally equivalent to driving a narrow single-photon transition.) Two-photon stimulated Raman transitions between the $|\downarrow\rangle$ and $|\uparrow\rangle$ states can be driven by tuning the difference frequency of R1 and R2 to be near ω_o. The two Raman beams ($\lambda \sim 313$ nm) are generated from a single laser source and acousto-optic modulator, allowing excellent stability of their relative frequency and phase. Both beams are detuned $\Delta/2\pi \approx 12$ GHz from the excited $^2P_{1/2}$ electronic state (radiative linewidth $\gamma/2\pi \approx 19.4$ MHz), and the polarizations are set to couple through the $^2P_{1/2}(F=2, m_F=2)$ level (the next nearest levels are the $^2P_{3/2}$ states which are over 200 GHz away and can be neglected). Because $\Delta \gg \gamma$, the excited ^2P state can be adiabatically eliminated in a theoretical description, resulting in a coupling between the two ground states which exhibits a linewidth inversely proportional to the interaction time. When R1 and R2 are applied to the ion with wavevector difference $\delta\vec{k} = \vec{k}_1 - \vec{k}_2$ along the x-direction, the effective coupling Hamiltonian in the rotating-wave approximation is given by

$$H_I = g\left(\sigma_+ e^{i\eta(a^\dagger + a) - i\delta t} + \sigma_- e^{-i\eta(a^\dagger + a) + i\delta t}\right). \tag{4}$$

The coupling strength g depends on Δ and the intensity of the laser beams, $\eta = |\delta\vec{k}|x_0 \sim 0.2$ is the Lamb-Dicke parameter, $x_0 = (\hbar/2m\omega)^{1/2} \approx 7$ nm, and δ is the difference between the relative frequency of the two Raman beams and ω_o. Setting $\delta\vec{k}$ to be parallel to the x-axis of the trap, yields almost no coupling between the internal states and motion in the y- and z-directions.

If $\delta = \omega(n'-n)$, transitions are resonantly driven between the levels $|\downarrow,n\rangle$ and $|\uparrow,n'\rangle$ at a rate $\Omega_{n,n'}$ which is dependent on n and n'[8]. Starting from the $|\downarrow\rangle|n\rangle$ state, application of a Rabi -π pulse coherently transfers the ion to the $|\uparrow\rangle|n'\rangle$ state; this corresponds to applying the Raman beams for a duration τ such that $\Omega_{n,n'}\tau = \pi/2$. If we apply the Raman beams for half of this time, we create the entangled state of Eq. (1). Here, we will assume the ion is confined in the Lamb-Dicke limit ($|\delta\vec{k}|\langle x^2\rangle^{1/2} \ll 1$) and will consider three transitions. The carrier, at $\delta = 0$, drives transitions between states $|\downarrow,n\rangle \leftrightarrow |\uparrow,n\rangle$ with Rabi frequency $\Omega_{n,n} = g$. The "first red sideband," corresponding to $\delta = -\omega$, drives transitions between states $|\downarrow,n\rangle \leftrightarrow |\uparrow,n-1\rangle$ with Rabi frequency $\Omega_{n,n-1} = g\eta\sqrt{n}$. This coupling is analogous to the case in cavity-QED[4] where energy is coherently exchanged between the internal and external degrees of freedom. The "first blue sideband," at $\delta = +\omega$, drives transitions between states $|\downarrow,n\rangle \leftrightarrow |\uparrow,n+1\rangle$ with Rabi frequency $\Omega_{n,n+1} = g\eta(n+1)^{1/2}$.

Preparation of the $|\downarrow\rangle|n=0\rangle$ state is accomplished by first Doppler cooling the ion to $\langle n\rangle \sim 1$, followed by sideband laser cooling using stimulated Raman transitions[11]. For sideband laser cooling, π pulses on the first red sideband ($|\downarrow\rangle|n\rangle \rightarrow |\uparrow\rangle|n-1\rangle$) are alternated with repumping cycles using nearly resonant radiation (Fig. 1b) - which results (most probably) in transitions $|\uparrow\rangle|n\rangle \rightarrow |\downarrow\rangle|n\rangle$. These steps are repeated (typically 5 times) until

the ion resides in the $|\downarrow\rangle|0\rangle$ state with high probability (> 0.9).

From the $|\downarrow\rangle|0\rangle$ state, we are able to coherently create states of the form $|\downarrow\rangle\Psi(x)$, where the motional state $\Psi(x) = \Sigma_n C_n e^{-i\omega_n t}|n\rangle$ and the C_n are complex. We can analyze the motional state created as follows: The Raman beams are pulsed on for a time τ and the probability $P_\downarrow(\tau)$ that the ion is in the $|\downarrow\rangle$ internal state is measured. The experiment is repeated for a range of τ values. When the Raman beams are tuned to the first blue sideband, the expected signal is

$$P_\downarrow(\tau) = \frac{1}{2}\left(1 + \sum_{n=0}^{\infty} P_n \cos(2\Omega_{n,n+1}\tau)e^{-\gamma_n \tau}\right), \tag{5}$$

where $P_n \equiv |C_n|^2$ is the probability of finding the ion in state n and γ_n are experimentally determined decay constants. The internal state $|\downarrow\rangle$ is detected by applying near-resonant σ^+-polarized laser radiation (beam D2, Fig. 1b) between the $|\downarrow\rangle$ and $^2P_{3/2}(F=3, m_F=3)$ energy levels. Because this is a cycling transition, detection efficiency is near unity[8,11]. The measured signal $P_\downarrow(\tau)$ can be inverted (Fourier cosine transform), allowing the extraction of the probability distribution of vibrational state occupation P_n. This signal does not show the phase coherences (phase factors of the C_n), which must be verified separately[8,12]. The most complete characterization is achieved with a state reconstruction technique[13].

3.2 Creation of Coherent and Schrödinger-Cat states

We have created and analyzed thermal, Fock, squeezed, coherent, Schrödinger-cat states, and superpositions of Fock states[8,12,13]; here we briefly describe the creation and measurements of coherent and Schrödinger-cat states. A coherent state of motion

$$\Psi(x) = |\alpha\rangle \equiv \exp(-|\alpha|^2/2)\sum_{n=0}^{\infty}\frac{\alpha^n}{\sqrt{n!}}|n\rangle, \tag{6}$$

corresponds to a displaced zero-point wave-packet oscillating in the potential well with amplitude $2|\alpha|x_0$. From Eq. (5), $P_\downarrow(\tau)$ for a coherent state will undergo quantum collapses and revivals[14]. These revivals are a purely quantum effect due to the discrete energy levels and the narrow distribution of states[4,14].

We have produced coherent states of ion motion from the $|\downarrow\rangle|0\rangle$ state by applying either a resonant (frequency ω) classical driving field or a "moving standing wave" of laser radiation which resonantly drives the ion motion through the dipole force[8,12]. In Fig. 2, we show a measurement of $P_\downarrow(\tau)$ after creation of a coherent state of motion, exhibiting the expected collapse and revival signature. (For comparison, see the cavity-QED experiment of Ref. 4.) This data is fitted to Eq. (5) assuming a Poissonian distribution, allowing only $\langle n\rangle$ to vary. The inset shows the results of a separate analysis, which yield the probabilities of the Fock-state components, extracted by applying a Fourier cosine transform to $P_\downarrow(\tau)$ at the known frequencies as described above. These amplitudes display the expected

Poissonian dependence on n.

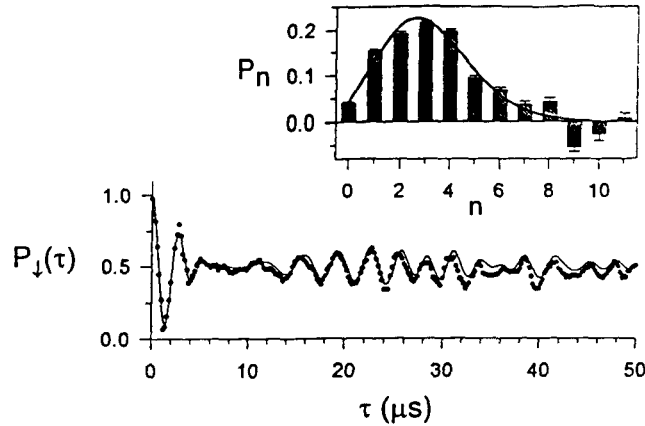Fig. 2. $P_{\downarrow}(\tau)$ for a coherent state driven by the first blue sideband interaction, showing collapse and revival behavior. The data are fitted to a coherent state distribution, yielding $\langle n \rangle = 3.1(1)$. The inset shows the results of inverting the time-domain data by employing a Fourier cosine transform at the known Rabi frequencies $\Omega_{n,n+1}$, fitted to a Poissonian distribution, yielding $\langle n \rangle = 2.9(1)$. Each data point represents an average of ≈ 4000 measurements, or 1 s of integration.

A Schrödinger-cat state is a coherent superposition of classical-like states. In Schrödinger's original thought experiment[15], he described how one could, in principle, entangle a superposition state of an atom with a macroscopic-scale superposition of a live and dead cat. In our experiment[12], we construct an analogous state, on a smaller scale, with a single atom. We create the state

$$\Psi = \frac{1}{\sqrt{2}}(|\downarrow\rangle|\alpha_1\rangle + e^{i\phi}|\uparrow\rangle|\alpha_2\rangle), \tag{7}$$

where $|\alpha_1\rangle$ and $|\alpha_2\rangle$ are coherent motional states and ϕ is a (controlled) phase factor. The coherent states of the superposition are spatially separated by mesoscopic distances much greater than the size of the atom wavepacket which has a spread equal to x_0.

Analysis of this state is interesting from the point of view of the "quantum measurement problem," an issue that has been debated since the inception of quantum theory by Einstein, Bohr, and others, and continues today[16]. One practical approach toward resolving this controversy is the introduction of quantum decoherence, or the environmentally induced reduction of quantum superpositions into classical statistical mixtures[17]. Decoherence provides a way to quantify the elusive boundary between classical and quantum worlds, and almost always precludes the existence of macroscopic Schrödinger-cat states, except at extremely short time scales. On the other hand, the creation of mesoscopic Schrödinger-cat states like that of Eq. (7) may allow controlled studies of quantum decoherence and the quantum-classical boundary. This problem is directly relevant to quantum computation.

In our experiment, we create a Schrödinger-cat state of the single-ion $^9Be^+$ harmonic oscillator (Eq. (7)) with a sequence of laser pulses[12]. First, we create a state of the form $(|\downarrow\rangle + e^{i\chi}|\uparrow\rangle)|n=0\rangle/\sqrt{2}$ with a $\pi/2$ pulse on the Raman carrier transition (Sec. 3.1). To spatially separate the $|\downarrow\rangle$ and $|\uparrow\rangle$ components of the wave function, we apply a coherent excitation with an optical dipole force which, because of the polarization of the beams used to create the force, selectively excites the motion of only the $|\uparrow\rangle$ state. We then swap the $|\downarrow\rangle$ and $|\uparrow\rangle$ states with a π-carrier pulse and reapply the dipole force with a different phase to create the state of Eq. (7). In principle, if we could make $|\alpha_{1,2}|$ large enough, we could design a detector which could directly detect the (distinguishable) position of the particle and correlate it with a spin measurement[18]. Instead, to analyze this state in our experiment, we apply an additional laser pulse to couple the internal states, and we measure the resulting interference of the distinct wavepackets. With this interferometer, we can establish the correlations inherent in Eq. (7), the separation of the wavepackets, and the phase coherence ϕ between components of the wavefunction. These experiments are described in Ref. 12. The interference signal should be very sensitive to decoherence. As the separation $|\alpha_1 - \alpha_2|$ is made larger, decoherence is expected to exponentially degrade the fringe contrast[4,17].

We remark that other experiments generate Schrödinger-cats in the same sense as in our experiment. Examples are atom interferometers[19,20], and superpositions of electron wavepackets in atoms[21] (also, see additional citations in Ref. 12). However, as opposed to these experiments, the harmonic oscillator cat states of Eq. (7) do not disperse in time. This lack of dispersion provides a simple visualization of the "cat" (e.g., a marble rolling back and forth in a bowl which can be simultaneously at opposite extremes of motion) and should allow controlled studies of decoherence models.

4   Quantum Logic

Interest in quantum computation in the atomic physics community was stimulated, in part, by a talk given by Artur Ekert at the last ICAP meeting[22]. Subsequently, Ignacio Cirac and Peter Zoller[23,24] proposed an attractive scheme for a quantum computer which would use a string of ions in a linear trap as "qubits." This proposal has stimulated experimental efforts in several laboratories including those at Innsbruck, Los Alamos National Laboratory, IBM, and NIST.

Each qubit in a quantum computer could be implemented by a two-level atomic system; for the ith qubit, we label these states $|\downarrow\rangle_i$ and $|\uparrow\rangle_i$ as above. In general, any quantum computation can be comprised of a series of single-bit rotations and two-bit "controlled-NOT" (CN) logic operations[22,25]. We are interested in implementing these two operations in a system of $^9Be^+$ ions. Single-bit rotations are straightforward and correspond to driving Raman carrier transitions (Sec. 3.1) for a controlled time. Such rotations have been achieved in many previous experiments. Next, we describe the demonstration of a nontrivial CN logic gate with a single $^9Be^+$ ion[26].

4.1   "Conditional dynamics" and a single-ion controlled-not logic gate

The key to making a quantum logic gate is to provide conditional dynamics; that is, we

desire to perform on one physical subsystem a unitary transformation which is conditioned upon the quantum state of another subsystem[22]. In the context of cavity QED, the required conditional dynamics at the quantum level has recently been demonstrated[27,28]. For trapped ions, conditional dynamics at the quantum level has been demonstrated in verifications of zero-point laser cooling[11,29]. Recently, we demonstrated a CN logic gate with the ability to prepare arbitrary input states (the "keyboard").

A two-bit quantum CN operation provides the transformation:

$$|\epsilon_1\rangle|\epsilon_2\rangle \rightarrow |\epsilon_1\rangle|\epsilon_1 \oplus \epsilon_2\rangle , \tag{8}$$

where $\epsilon_1, \epsilon_2 \in \{0,1\}$ and $\oplus$ is addition modulo 2. The (implicit) phase factor in the transformation is equal to 1. In this expression ϵ_1 is the called the control bit and ϵ_2 is the target bit. If $\epsilon_1 = 0$, the target bit remains unchanged; if $\epsilon_1 = 1$, the target bit flips. In the single-ion experiment of Ref. 26, the control bit is the quantized state of one mode of the ion's motion. If the motional state is $|n=0\rangle$, it is taken to be a $|\epsilon_1=0\rangle$ state; if the motional state is $|n=1\rangle$, it is taken to be a $|\epsilon_1=1\rangle$ state. The target states are two ground-hyperfine states of the ion, the $|\downarrow\rangle$ and $|\uparrow\rangle$ states of Sec. 3.1 with the identification here $|\downarrow\rangle \rightarrow |\epsilon_2=0\rangle$ and $|\uparrow\rangle \rightarrow |\epsilon_2=1\rangle$. Following the notation of Sec. 3.1, the CN operation is realized by applying three Raman laser pulses in succession:

(1a)   A "$\pi/2$-pulse" is applied on the spin carrier transition. For a certain choice of initial phase, this corresponds to the operator $V^x(\pi/2)$ of Ref. 23.

(1b)   A 2π-pulse is applied on the first blue sideband transition between levels $|\uparrow\rangle$ and an auxiliary level $|aux\rangle$ in the ion (the $|F=2, M_F=0\rangle$ level in $^9Be^+$). This operator is analogous to the operator U_x^{21} of Ref. 23. This operation provides the conditional dynamics for the controlled-not operation in that it changes the sign of the $|\uparrow\rangle|n=1\rangle$ component of the wavefunction but leaves the sign of the $|\uparrow\rangle|n=0\rangle$ component of the wavefunction unchanged.

(1c)   A $\pi/2$-pulse is applied to the spin carrier transition with a 180° phase shift relative to step (1a). This corresponds to the operator $V^x(-\pi/2)$ of Ref. 23.

Steps (1a) and (1c) can be regarded as two resonant pulses (of opposite phase) in the Ramsey separated-field method of spectroscopy. We can see that if step (b) is active (thereby changing the sign of the $|\uparrow\rangle|n=1\rangle$ component of the wave function) then a spin flip is produced by the Ramsey fields. If step (1b) is inactive, the net effect of the Ramsey fields is to leave the spin state unchanged. This CN operation can be incorporated to provide an overall CN operation between two ions in an ensemble of N ions if we choose the ion oscillator mode to be the center-of-mass (COM) mode of the ensemble. Specifically, to realize a controlled-not $C_{m,k}$ between two ions (m = control bit, k = target bit), we first assume the COM is prepared in the zero-point state. The initial state of the system is therefore given by

$$\Psi = \left(\sum_{i=1}^{N} \sum_{M_i=1,1} C_{M_1,M_2,...M_N} |M_1\rangle_1 |M_2\rangle_2 ... |M_N\rangle_N \right) |0\rangle . \qquad (9)$$

$C_{m,k}$ can be accomplished with the following steps:

(2a) Apply a π-pulse on the red sideband of ion m (the assumption is that ions can be addressed separately[23]). This accomplishes the mapping $(\alpha|\downarrow\rangle_m + \beta|\uparrow\rangle_m)|0\rangle \rightarrow$ $|\downarrow\rangle_m(\alpha|0\rangle - e^{i\phi}\beta|1\rangle)$, and corresponds to the operator $U_m^{1,0}$ of Ref. 23. We note that in our experiments, we prepare the state $(\alpha|\downarrow\rangle + \beta|\uparrow\rangle)|0\rangle$ using the carrier transition (Sec. 3.1). We can then implement the mapping $(\alpha|\downarrow\rangle + \beta|\uparrow\rangle)|0\rangle \rightarrow$ $|\downarrow\rangle_m(\alpha|0\rangle - e^{i\phi}\beta|1\rangle)$. This is the "keyboard" operation for preparation of arbitrary motional input states for the CN gate of steps 1a - 1c above. Analogous mapping of internal state superpositions to motional state superpositions were demonstrated in Ref. 26.

(2b) Apply the CN operation (steps 1a - 1c above) between the COM motion and ion k.

(2c) Repeat step (2a).

Overall, $C_{m,k}$ provides the mappings $|\downarrow\rangle_m|\downarrow\rangle_k|0\rangle \rightarrow |\downarrow\rangle_m|\downarrow\rangle_k|0\rangle$, $|\downarrow\rangle_m|\uparrow\rangle_k|0\rangle \rightarrow |\downarrow\rangle_m|\uparrow\rangle_k|0\rangle$, $|\uparrow\rangle_m|\downarrow\rangle_k|0\rangle \rightarrow |\uparrow\rangle_m|\uparrow\rangle_k|0\rangle$,and $|\uparrow\rangle_m|\uparrow\rangle_k|0\rangle \rightarrow |\uparrow\rangle_m|\downarrow\rangle_k|0\rangle$ which is the desired logic of Eq. (8). Effectively, $C_{m,k}$ works by mapping the internal state of ion m onto the COM motion, performing a CN between the motion and ion n, and then mapping the COM state back onto ion m. The resulting CN between ions m and k is not really different from the CN described by Cirac and Zoller[7], because the operations $V^{\kappa}(\theta)$ and $U_m^{1,0}$ commute.

4.2   Quantum Registers and Schrödinger Cats

The state represented by Eq. (9) is of the same form as that of Eq. (7). Both involve entangled superpositions and both are subject to the destructive effects of decoherence. Creation of Schrödinger-cats like Eq. (7) is particularly relevant to the ion-based quantum computer because the primary source of decoherence will probably be due to decoherence of the $|n=0,1\rangle$ motional states during the logic operations.

5   Potential for, and Problems with, Trapped-Ion Quantum Logic

Quantum computation has received a great deal of attention recently because of the algorithm proposed by Peter Shor for efficient factorization[30]. This has important implications for public-key data encryption where the security of these systems is due to the inability to efficiently factorize large numbers. To accomplish quantum factorization is extremely formidable with any technology; however, other applications of quantum logic may be more tractable.

5.1   Positive Aspects of Trapped-Ion Quantum Logic

Internal state decoherence can be relatively small in experiments on trapped ions. The ions' energy level structure is, of course, perturbed at some level by electric and magnetic fields. However, energy level shifts caused by electric fields (Stark shifts) tend to be quite small and, in many cases, level shifts due to magnetic fields can be controlled well enough. This is evident from trapped-ion atomic clock experiments where linewidths smaller than 0.001 Hz have been achieved[31,32], indicating internal state coherence times exceeding 10 min.

The required laser cooling to $|n=0\rangle$ has been demonstrated[11,29] for single ions. A string of laser-cooled ions (Fig. 3), which could be used as a quantum register, has been achieved in a linear ion trap[33,34], but an immediate future task will be to achieve zero-point cooling (for at least the COM mode) on an ensemble of ions. For a computation performed on an ensemble of ions in a trap, this need not be done extremely well. All we require is that the cooling be sufficient that the ion's COM mode is predominantly in the n=0 state, so the "correct" answer to a computation is obtained most of the time. Similarly, although nearly unit detection efficiency has been achieved with trapped ions[11,35], the basic requirement is that the noise in the "readout" of the quantum register should minimize the number of times the calculation is repeated.
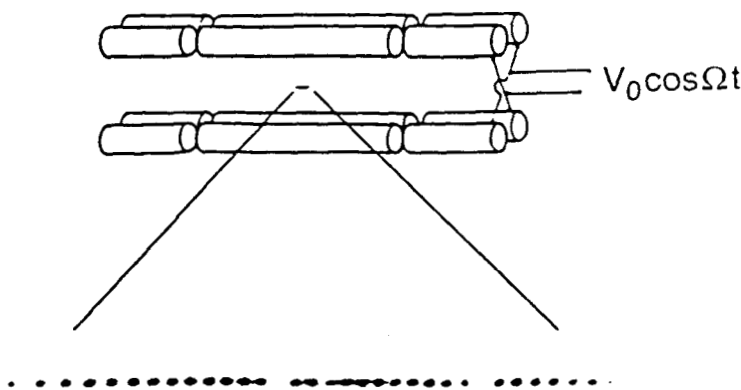

Fig. 3. The upper part of the figure shows a schematic diagram of the electrode configuration for a linear Paul-RF trap (rod spacing ~ 1 mm)[34]. The lower part of the figure shows an image of a string of [199]Hg^{+} ions, illuminated with 194 nm radiation, taken with a UV-sensitive, photon counting imaging tube. The spacing between adjacent ions is approximately 10 μm. The "gaps" in the string are occupied by impurity ions, most likely other isotopes of Hg^{+}, which do not fluoresce because the frequencies of their resonant transitions do not coincide with those of the 194 nm $^2S_M \rightarrow {}^2P_M$ transition of [199]Hg^{+}.

Estimates of motional decoherence times from the $|n=0,1\rangle$ states, due to fundamental causes, should be very long (more than 100 s)[36]. However, these predictions have not been realized experimentally and the causes of the observed decoherence[11,29] must still be found.

5.2   *Problems and Possible Solutions*

Many problems may conspire to prevent large-scale quantum computation; some of the problems relevant to trapped ions are briefly mentioned here. More complete analyses are given elsewhere,[37, 38].

Motional decoherence can arise from fluctuating trap fields and radiative coupling to the environment. The integrity of the trap electrode structure is expected to play an important role, particularly if the number of ion qubits becomes large. Lithographic techniques for constructing electrodes[39] may be useful to insure accurate dimensional tolerances. With these techniques, it may also be possible to incorporate accurate (Josephson) voltage standards and (superconducting) flux magnetometers into the structure.

Laser power fluctuations will affect the fidelity of the rotations and logic gates (for example, $\pi/2$ rotations become $\pi/2 \pm \epsilon$ rotations where ϵ is unknown). Although the effects depend on the form of the noise and on the computational algorithm, a conservative estimate is to assume that phase errors accumulate linearly with the number of elemental operations. A computation requiring 10^6 elemental operations would therefore require an intensity stability of one part in 10^6 over the time of the computation. With current algorithms, factorization of large numbers will require even more elemental operations, so extreme laser stabilization will be required.

We have noted some of the advantages of using stimulated Raman transitions in quantum logic[26]. One apparent disadvantage is that, since the Raman beams are detuned from a virtual optical level, the energy levels are shifted by AC-Stark effects [see for example Ref. 36]. These effects are absent in single-photon transitions as assumed in Ref. 23. Therefore, if stimulated-Raman transitions are used and if the laser intensities fluctuate, additional Stark-induced phase errors will accumulate. However, we can show[38] that these errors are of the same order as those incurred from the angular errors of the preceding paragraph, if the two Raman laser intensities are approximately equal.

The scheme of Cirac and Zoller[23] assumes that the laser beams can separately address individual ion qubits. This necessitates a tradeoff between two factors. We desire that the ions be well separated spatially to allow a focused laser beam to address only one ion at a time. However, we also desire to spectrally isolate individual modes of the ion motion, to insure the fidelity of the logic. The closer in frequency the "contaminating" transitions (from coupling to other motional modes) are, the slower the logic speed must be to obtain isolation. To give an idea of the problem, we note that the separation of two $^9\text{Be}^+$ ions confined in a harmonic well of frequency $\nu = \omega/2\pi$ is given by $d = 9.21\nu^{-2/3}$ where d is in micrometers and ν in megahertz. For longer strings, the spacing of the central ions becomes closer[40]. Although the focusing predicted with the use of Gaussian beam formulas implies the required isolation could be obtained for ν up to a few MHz, in practice, stray light intensity will undoubtedly be a problem. With the use of stimulated-Raman transitions [26,36], one solution for this problem is to take advantage of the inherent AC Stark shifts. The basic idea is that the (resonant) Rabi frequencies g_1, g_2 of the two Raman beams are made substantially different, say $g_1 >> g_2$. The transition frequency for the selected qubit is therefore shifted from the frequency of adjacent ions so that the adjacent ions are relatively unaffected. Unfortunately, the sensitivity to intensity fluctuations also becomes worse by the

ratio g_1/g_2[38].

A large scale computation will require a large qubit register. This makes it extremely hard to isolate unwanted motional mode transitions from the desired one[38]. As noted in Ref. 23, the desired COM trap-axis mode frequency in a linear trap is smaller than other trap axis modes and can therefore be relatively well isolated spectrally. However, as the number of ions in the trap increases, the radial mode frequencies will tend to overlap the COM mode frequency. Also, multi-mode excitations may become a problem when the difference frequency of the modes is close to the COM mode frequency. Therefore, a multiplexing scheme for ion qubit registers seems desirable; we discuss one possibility below.

5.3 A 1- or 2-qubit ion accumulator

One possibility for multiplexing in a trapped-ion quantum computer is to perform all logic in minimal accumulators which hold one or two ions at a time[38]. Ions would be shuffled around in a "super-register" and into and out of the accumulators which are well shielded from the other ions. The shuffling could be accomplished with interconnected linear traps with segmented electrodes; this appears possible with the use of lithographic techniques. Single-bit rotations on the mth ion would be accomplished by moving that ion into an accumulator. Logic operations between ions m and k would be accomplished by first moving these ions into an accumulator. An accumulator would hold a second species of ion (say Mg^+) which could be used to provide laser cooling to the $|n=0\rangle$ level (of the mode used for the gate) if necessary. Therefore, for logic operations, an accumulator would hold two computational ions and the auxiliary ion. This scheme should make it easier to select ions with laser beams because it should be straightforward to address one ion while nulling the laser intensity on the other ion, even with very high trap frequencies. The very small number of logic ions in an accumulator (1 or 2) would make extraneous mode coupling much easier to avoid. The main problem appears to be that computational speed is reduced because of the time required to shuffle ions in and out of the accumulator and provide laser cooling with the auxiliary ion, if required. However, energy shifts of the ion's internal structure, due to the electric fields required to move the ion, need not be severe . For example, to move a $^9Be^+$ from rest to a location 1 cm away (and back to rest) in 1 μs would require a field of less than 50 V/cm. Electric fields of this order should give negligible phase shifts in qubits based on hyperfine structure[41]. The phase shift caused by time dilation would be less than 1 μrad.

5.4 Perspective on Ion Quantum Computation

To be useful for factorization, a quantum computer must be able to factorize a 200 digit decimal number. This will require a few thousand ions and perhaps 10^9 elementary operations[22]. Given the current state-of-the art (one ion and about 10 operations), we should therefore be skeptical. Decoherence will be most decisive in determining the fate of quantum computation. Already, decoherence from spontaneous emission appears to limit the number of operations possible[42,43]. The experiments can be expected to improve

dramatically, but we must hope for more efficient algorithms or ways to patch them (such as error correction schemes[24]) before large scale factorization is possible.

Any quantum system that might be contemplated in quantum computation must be reproducible, stable, and well isolated from the environment. Quantum dots have the potential advantage of large scale integration using microfabrication; however at the present time, they suffer from lack of precise reproducibility and excessive decoherence. Trapped ions are reproducible and relatively immune to environmental perturbations - this is the reason they are candidates for advanced frequency standards[44]. In principle, high information density could be achieved by scaling down the electrodes; however, we must then worry about excessive environmental coupling such as magnetic field perturbations caused by impurities and/or currents in the (nearby) trap electrodes[38]. Electric field perturbations will also become important. Therefore, in terms of scale, the trapped ion system may be close to optimum.

Finally, factorization, discrete logs, and certain other mathematical computations appear to be the hardest problems that quantum logic might be applied to. One of the applications for quantum computation that Richard Feynman originally had in mind was to simulate quantum mechanical calculations[45]. This idea is being explored again with new possibilities in mind[46]. Below, we consider an application to atomic measurement.

6   Quantum Logic Applied to Spectroscopy

We conclude by discussing a possible application of quantum logic in the realm of atomic physics. This application has the advantage of being useful with a relatively small number of ions and logic operations.

Entangled atomic states can improve the quantum-limited signal-to-noise ratio in spectroscopy[6,36,47]. In spectroscopy experiments on N atoms, in which changes in atomic populations are detected, we can view the problem in the following way using the spin-$\frac{1}{2}$ analogy for two-level atoms. We assume spectroscopy is performed by applying (classical) fields of frequency ω_R for a time T_R according to the Ramsey method of separated fields[48]. After applying these fields, we measure the final state populations. For example, we might measure the operator $\tilde{N}_-$ corresponding to the number of atoms in the $|\downarrow\rangle$ state. In the spin-$\frac{1}{2}$ analog, this is equivalent to measuring the operator J_z, since $\tilde{N}_- = J\tilde{I} - J_z$ where $\tilde{I}$ is the identity operator.

If all technical sources of noise are eliminated, the signal-to-noise ratio (for repeated measurements) is fundamentally limited by the quantum fluctuations in the number of atoms which are observed to be in the $|\downarrow\rangle$ state. These fluctuations can be called quantum "projection" noise[49]. If spectroscopy is performed on N initially uncorrelated atoms (e.g., $\Psi(t=0) = \Pi_i|\downarrow\rangle_i$), the imprecision in a determination of the frequency of the transition is limited by projection noise to $(\Delta\omega)_{meas.} = 1/(NT_R\tau)^{\frac{1}{2}}$ where $\tau \gg T_R$ is the total averaging time. If the atoms can be initially prepared in entangled states, it is possible to achieve $(\Delta\omega)_{meas.} < 1/(NT_R\tau)^{\frac{1}{2}}$. Initial theoretical investigations[6,36] examined the use of correlated states which could achieve $(\Delta\omega)_{meas.} < 1/(NT_R\tau)^{\frac{1}{2}}$ when the population (J_z) was measured. More recent theoretical investigations[47] consider the initial state to be one where, after the first Ramsey pulse, the internal state is the maximally entangled state of Eq. (2).

After applying the Ramsey fields, we measure the operator $\hat{O} = \Pi_i \sigma_{xi}$ instead of J_z (or $\hat{N}$). For unit detection efficiency, we can achieve $(\Delta\omega)_{min} = 1/(N^2 T_R \tau)^{\frac{1}{2}}$ which is the maximum signal-to-noise ratio possible. For an atomic clock where T_R is fixed by other constraints, this means that the time required to reach a certain measurement precision (stability) is reduced by a factor of N relative to the uncorrelated-atom case. In terms of quantum computation, this amounts to a computation of the function $\cos(N(\omega - \omega_o)T)$. Of course, this computation has special significance for the measurement of ω_o (an intrinsic computer parameter) but otherwise is much better suited for a classical computer! See Ref. 50 for related work.

Cirac and Zoller[23] have outlined a scheme for producing the state in Eq.(2) using quantum logic gates. Using the notation of Sec. 3.1, we would first apply a $\pi/2$ rotation to ion 1 to create the state $\Psi = 2^{-\frac{1}{2}}(|\downarrow\rangle_1 + e^{i\phi}|\uparrow\rangle_1)|\downarrow\rangle_2|\downarrow\rangle_3...|\downarrow\rangle_N$. We then apply the CN gate of Eq. (8) sequentially between ion 1 and ions 2 through N to achieve the state of Eq. (2). An alternative method for generating this state, without the need of addressing individual ions is described in Ref. 47.

Acknowledgments

References

†   Contribution of NIST; not subject to US copyright.

1.   A. Einstein, B. Podolsky, N. Rosen, *Phys. Rev.* **47**, 777 (1935).

2.   H. Dehmelt, *Science* **247**, 539 (1990).

3.   *Cavity Quantum Electrodynamics*, ed. by P.R. Berman (Academic Press, Boston, 1994).

4.   S. Haroche, et al., these proceedings.

5.   C.A. Blockley, D.F. Walls, and H. Risken, *Europhys. Lett.* **17**, 509 (1992).

6.   D. J. Wineland, J. J. Bollinger, W. M. Itano, F. L. Moore, and D. J. Heinzen, *Phys. Rev.* A**46**, R6797 (1992).

7.   J.I. Cirac, R. Blatt, A.S. Parkins, and P. Zoller, *Phys. Rev. Lett.* **70**, 762 (1993).

8.   D.M. Meekhof, C. Monroe, B.E. King, W.M. Itano, and D.J. Wineland, *Phys. Rev. Lett.* **76**, 1796 (1996).

9.   J.I. Cirac, A.S. Parkins, R. Blatt, P. Zoller, in *Adv. Atomic and Molecular Phys.*, to be published.

10.   S. R. Jefferts, C. Monroe, E. W. Bell, and D. J. Wineland, *Phys. Rev.* A**51**, 3112-3116 (1995).

11.   C. Monroe, D. M. Meekhof, B. E. King, S. R. Jefferts, W. M. Itano, D. J. Wineland, and P. Gould, *Phys. Rev. Lett.* **75**, 4011 (1995).

12.   C. Monroe, D. M. Meekhof, B. E. King, and D. J. Wineland, *Science* **272**, 1131

(1996).

13. D. Leibfried, D.M. Meekhof, B.E. King, C. Monroe, W.M. Itano, and D.J. Wineland, submitted.

14. J.H. Eberly, N.B. Narozhny, and J.J. Sanchez-Mondragon, *Phys. Rev. Lett.* **44**, 1323 (1980).

15. E. Schrödinger, *Naturwissenschaften* **23**, 807 (1935).

16. *Quantum Theory and Measurement*, ed. by J.A. Wheeler, W.H. Zurek (Princeton Univ. Press, Princeton, 1983).

17. W.H. Zurek, *Physics Today*, **44**, 36 (1991).

18. J.F. Poyatos, J.I. Cirac, R. Blatt, P. Zoller, *Phys. Rev.* A, to be published.

19. D.E. Pritchard, et al., these proceedings.

20. O. Carnal and J. Mlynek, *Phys. Rev. Lett.* **66**, 2689 (1991); D.W. Keith, C.R. Ekstrom, Q.A. Turchette, D.E. Pritchard, *Phys. Rev. Lett.* **66**, 2693 (1991); M. Kasevich and S. Chu, *Phys. Rev. Lett.* **67**, 181 (1991); J. Lawall, S. Kulin, B. Saubamea, N. Bigelow, M. Leduc, and C. Cohen-Tannoudji, *Phys. Rev. Lett.* **75**, 4194 (1995).

21. L.D. Noordam, D.I. Duncan, T.F. Gallagher, *Phys. Rev.* A**45**, 4734 (1992); R.R. Jones, C.S. Raman, S.W. Schumacher, P.H. Bucksbaum, *Phys. Rev. Lett.* **71**, 2575 (1993); M.W. Noel and C.R. Stroud, Jr., *Phys. Rev. Lett.* **75**, 1252 (1995).

22. A. Ekert, in *Atomic Physics 14*, ed. by D. J. Wineland, C. E. Wieman, and S. J. Smith, (proc. 14th International Conference on Atomic Physics, Boulder, CO, August, 1994), (AIP Press, NY, 1995), p. 450; A. Ekert and R. Jozsa, *Rev. Mod. Phys.*, July, 1996, to be published.

23. J.I. Cirac and P. Zoller, *Phys. Rev. Lett.* **74**, 4091 (1995).

24. P. Zoller, et al., these proceedings.

25. D.P. DiVincenzo, *Phys. Rev.* A**51**, 1051 (1995).

26. C. Monroe, D. M. Meekhof, B. E. King, W. M. Itano, and D. J. Wineland, *Phys. Rev. Lett.* **75**, 4714 (1995).

27. M. Brune, P. Nussenzveig, F. Schmidt-Kaler, F. Bernardot, A. Maali, J.M. Raimond, and S. Haroche, *Phys. Rev. Lett.* **72**, 3339 (1994).

28. Q. Turchette, C. Hood, W. Lange, H. Mabushi, H.J. Kimble, *Phys. Rev. Lett.* **75**, 4710 (1995).

29. F. Diedrich, J.C. Bergquist, W. M. Itano, and D.J. Wineland, *Phys. Rev. Lett.* **62**, 403 (1989).

30. P. Shor, Proc. 35th Ann. Symp. on the Foundations of Comp. Sci. (IEEE Comp. Soc. Press, NY, 1994). p. 124.

31. J. J. Bollinger, D. J. Heinzen, W. M. Itano, S. L. Gilbert, and D. J. Wineland, *IEEE Trans. on Instrum. and Meas.* **40**, 126 (1991).

32. P.T.H. Fisk, M.J. Sellars, M.A. Lawn, C. Coles, A.G. Mann, and D.G. Blair, *IEEE Trans. Instrum. Meas.* **44**, 113 (1995).

33. M. G. Raizen, J. M. Gilligan, J. C. Bergquist, W. M. Itano, and D. J. Wineland, *Phys. Rev.* A**45**, 6493 (1992).

34. J. Miller, M. E. Poitzsch, F. C. Cruz, D. J. Berkeland, J. C. Bergquist, W. M. Itano. and D. J. Wineland, Proc., 1995 IEEE Intl. Frequency Control Symp., June

1995, pp. 110-112; M. E. Poitzsch, J. C. Bergquist, W. M. Itano, and D. J. Wineland, *Rev. Sci. Instrum.* 67, 129 (1996).

35.   W. Nagourney, J. Sandberg, and H.G. Dehmelt, *Phys. Rev. Lett.* 56, 2797 (1986); Th. Sauter, R. Blatt, W. Neuhauser, and P.E. Toschek, *Phys. Rev. Lett.* 57, 1696 (1989); J.C. Bergquist, R.G. Hulet, W.M. Itano, and D.J. Wineland, *Phys. Rev. Lett.* 57, 1699 (1986).

36.   D.J. Wineland, J. J. Bollinger, W. M. Itano, and D. J. Heinzen, *Phys. Rev.* A50, 67 (1994).

37.   R.J. Hughes, D.F.V. James, E.H. Knill, R. Laflamme, and A.G. Petschek, Los Alamos report LA-UR-96-1266 (1966) (submitted to PRL); Los Alamos eprint archive quant-ph/9604026.

38.   D.J. Wineland, et al., in preparation.

39.   R. Brewer, R.G. DeVoe, and R. Kallenbach, *Phys. Rev.* A46, R6781 (1992).

40.   D. J. Wineland, J. C. Bergquist, J. J. Bollinger, W. M. Itano, D. J. Heinzen, S. L. Gilbert, C. H. Manney, and M. G. Raizen, *IEEE Trans. on Ultrasonics, Ferroelectrics, and Frequency Control* 37, 515 (1990).

41.   Wayne M. Itano, L.L. Lewis, and D.J. Wineland, *Phys. Rev.* A25, 1233 (1982).

42.   M.B. Plenio and P.L. Knight, Phys. Rev. A53, 2986 (1996).

43.   We note that the effects of spontaneous emission are significantly reduced if rf transitions between hyperfine levels are induced with inhomogeneous rf fields (Sec. 3).

44.   see: *Proc., Fifth Symp. Freq. Standards and Metrology*, ed. by J.C. Bergquist, Woods Hole, MA, Oct. 1995 (World Scientific, Singapore, 1996).

45.   R.P. Feynman, *Int. J. Theor. Phys.* 21, 467 (1982); *Opt. News* 11, 11 (1985); *Found. Phys.* 16, 507 (1986).

46.   S. Lloyd, *Science*, to be published.

47.   J. J. Bollinger, D. J. Wineland, W. M. Itano, and D. J. Heinzen, *Proc., Fifth Symp. Freq. Standards and Metrology*, ed. by J.C. Bergquist, Woods Hole, MA, Oct. 1995 (World Scientific, Singapore, 1996), p. 107.

48.   N.F. Ramsey, *Molecular Beams*, (Oxford University Press, London, 1963).

49.   W. M. Itano, J. C. Bergquist, J. J. Bollinger, J. M. Gilligan, D. J. Heinzen, F. L. Moore, M. G. Raizen, and D. J. Wineland, *Phys. Rev.* A47, 3554 (1993).

50.   J. Sørensen, J Erland, J. Hald, A. Kuzmich, K. Mølmer, and E.S. Polzik, contributed abstract, this meeting.